

### CHAPTER III

#### OPTICAL AND MAGNETIC STUDIES OF DIVALENT $3d^6$ ION DOPED IN $\text{CsCdCl}_3$ AT LOW TEMPERATURE

We studied the polarized absorption spectra and magnetic susceptibility and anisotropy of  $\text{Fe}^{2+}$  ( $3d^6$ ) in  $\text{CsCdCl}_3$  only. We had to leave out the investigation of  $\text{CsCdCl}_3 : \text{Cr}^{2+}$  ( $3d^4$ ) crystal which we prepared, as the valence state of chromium here was uncertain due to easy oxidation of  $\text{Cr}^{2+}$ .

#### RESULTS AND DISCUSSION

##### I. Optical Studies

The electronic ground state of the free  $\text{Fe}^{2+}$  ion is  $^5D$ , which is incidentally the only quintet term for the  $d^6$  configuration. An octahedral crystalline field splits the state into an upper orbital doublet  $^5E_g$  and a lower orbital triplet  $^5T_{2g}$  (Fig. 12). The only spin allowed transition for  $\text{Fe}^{2+}$  involves these two states and the separation between them gives the measure of  $10 Dq$ . The small trigonal field present in  $C_{3v}$  sites of  $\text{CsCdCl}_3$ , splits the lower triplet further into a singlet  $^5A_1 (C_{3v})$  and a doublet  $^5E (C_{3v})$  leaving the upper  $^5E_g (O_h)$  unsplit. The upper state might be split by the spin-orbit interaction or by the combined action of the trigonal field and spin-orbit interaction, but such splitting is expected to be small compared to Jahn-Teller splitting. For  $\text{Fe}^{2+}$  in crystalline field ( $O_h$  symmetry) it has been shown<sup>82</sup> that the magnitude of the Jahn-Teller splitting is at least 10 times greater for the upper  $^5E_g$  than

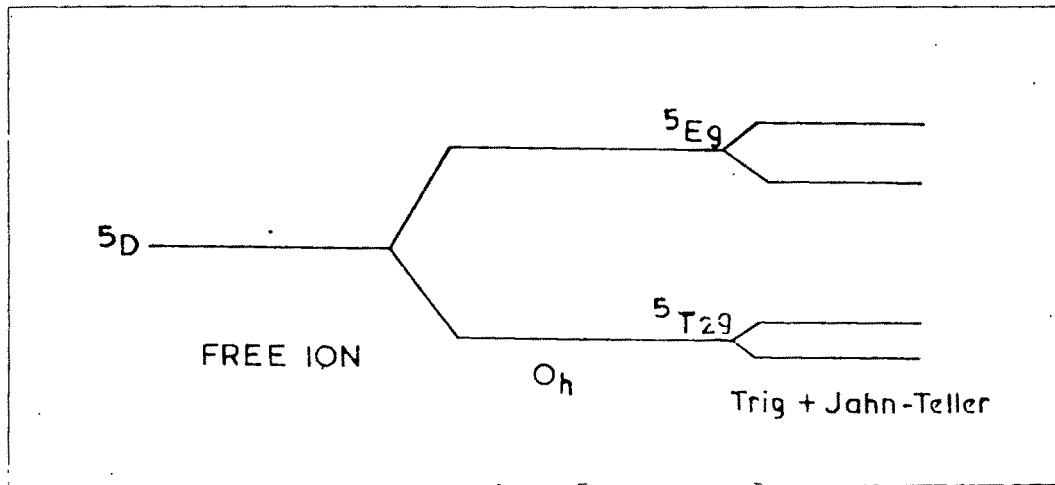


Fig.12. Splitting of  $5D$  term of  $Fe^{2+}$  in  $CsCdCl_3$

for the  ${}^5T_{2g}$  ground state and thus to a good approximation, the Jahn-Teller splitting of the  ${}^5T_{2g}$  ground state may be neglected. In an octahedral complex having Jahn-Teller coupling to just one vibration mode  $\omega$ , the splitting  $\Delta\omega$  for the upper  ${}^5E_g$  state is given by Sturge<sup>73</sup>

$$\Delta\omega = 2(\Delta E \hbar\omega)^{1/2} = (2\hbar A^2/m\omega)^{1/2} \quad (91)$$

where  $\Delta E = (A^2/2m\omega^2)$  is the J-T stabilization energy and  $A$  is a parameter representing the magnitude of Jahn-Teller coupling. For trigonally symmetric compounds, the only electronic levels remaining degenerate are the doubly degenerate E levels and the Jahn-Teller interaction is that of an E-electronic level with an e-vibrational mode. Both the electronic level and e-vibrational mode are unaffected by the trigonal field. And as no new features are introduced due to lowering of symmetry from the cubic case, the above formula can be applied.

From our room temperature spectrum (Fig. 13 dotted line) we assigned the absorption band at  $6450 \text{ cm}^{-1}$  for  ${}^5T_{2g} \rightarrow {}^5E_g$  transition and calculated the observed Dq to be  $\sim 645 \text{ cm}^{-1}$ . This is low in comparison with Dq of  $\text{Fe}^{2+}$  in oxides ( $1030 \text{ cm}^{-1}$ )<sup>143</sup> and hydroxides ( $\sim 1000 \text{ cm}^{-1}$ )<sup>144</sup>. But it is close to Dq observed in  $\text{CdCl}_2 : \text{Fe}^{2+}$  ( $660 \text{ cm}^{-1}$  at  $81^\circ\text{K}$ ) by Freeman and Jones<sup>76</sup>. As in  $\text{CsCdCl}_3 : \text{Co}^{2+}$ , this low value is obviously due to large Fe-Cl distance ( $\sim 2.6 \text{ \AA}$ ) in the present crystal (i.e. due to the large difference in the ionic radii of  $\text{Fe}^{2+}$  ( $0.83 \text{ \AA}$ ) and substituted  $\text{Cd}^{2+}$  ( $1.03 \text{ \AA}$ ) as well as the greater magnitudes of

ligand fields in oxide and hydroxide complexes. It is also observed that  $Dq$  is much smaller than theoretical  $9/4$  of the tetrahedral  $Dq$  in  $FeCl_4^-$  ( $510\text{ cm}^{-1}$ )<sup>145</sup> in chloride melt (KCl - LiCl).

The absorption spectrum at  $77^\circ\text{K}$  (Fig. 13a solid line) shows that  ${}^5T_{2g} \rightarrow {}^5E_g$  band splits into two components at  $5210\text{ cm}^{-1}$  and  $6370\text{ cm}^{-1}$ . This splitting we ascribe to the Jahn-Teller distortion of the upper  ${}^5E_g$  states. The lack of polarization of the bands agrees with this assignment. The separation  $1160\text{ cm}^{-1}$ , of the components, which measures the magnitude of the Jahn-Teller distortion is much less than that observed for  $Fe^{2+}$  surrounded by a distorted octahedral of  $OH^-$  ions ( $2000\text{ cm}^{-1}$ ) by Liehr and Ballhausen<sup>146</sup>. But this splitting is comparable to the Jahn-Teller splittings observed in  $CdCl_2 : Fe^{2+}$  ( $935\text{ cm}^{-1}$ ) at  $81^\circ\text{K}$ ;  $CdBr_2 : Fe^{2+}$  ( $765\text{ cm}^{-1}$ ) at  $81^\circ\text{K}$ ;  $MgCl_2 : Fe^{2+}$  ( $885\text{ cm}^{-1}$ ) at  $82^\circ\text{K}$ ; and  $FeCl_2$  ( $970\text{ cm}^{-1}$ ) at  $83^\circ\text{K}$  by Freeman and Jones<sup>76</sup>. According to Sturge<sup>73</sup> this splitting is temperature dependent.

In addition to the above transitions, we have observed at room temperature a band at  $25040\text{ cm}^{-1}$  (Fig. 13b) with high extinction coefficient. Since for  $d^6$  configuration, there is no other term near  ${}^5T_{2g}$ , we should ascribe this to a charge-transfer transition of an electron from Cl-ligand to central metal ion. Constructing the molecular-orbital energy level scheme for an octahedral complex it can be seen that all the bonding and non-bonding ligand orbitals (Fig. 14a)  $a_{1g} (\sigma^b)$ ,  $e_g (\sigma^b)$ ,  $t_{1u} (\sigma^b)$ ,  $t_{2g} (\pi^b)$ ,  $t_{1u} (\pi^b)$ ,  $t_{2u} (\pi^b)$  and  $t_{1g} (\pi^b)$  are

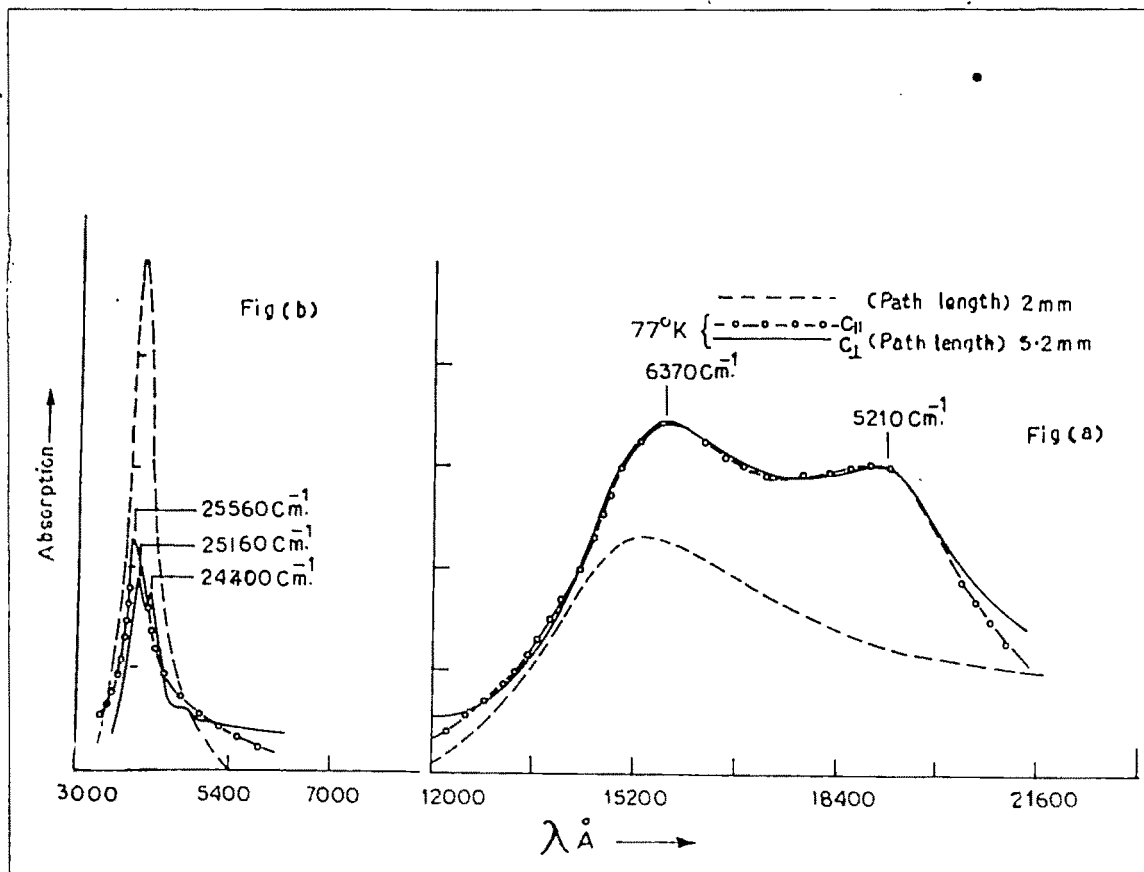


Fig.13. Absorption spectrum of  $\text{Fe}^{2+}$  in  $\text{CsCdCl}_3$ . The dotted line is the unpolarized room temperature spectrum. The chain and solid line is the polarized spectrum at  $77^\circ\text{K}$ .

Fig.(a) shows the d-d band and Fig.(b) shows the charge-transfer band (path length 0.5 mm).

filled and our observed charge-transfer band should correspond to  $t_{2u}$  (ligand)  $\rightarrow$   $t_{2g}$  (metal orbital)\*. Under  $C_{3v}$ , metal  $t_{2g}$  orbital breaks into  $e$  ( $t_{2g}$ ) and  $a_1$  ( $t_{2g}$ ) and the  $t_{2u}$  ligand orbital into  $e$  ( $t_{2u}$ ) and  $a_1$  ( $t_{2u}$ ). In parametric fittings of our magnetic susceptibilities and anisotropies we have seen that if we consider +ve values of  $\Delta$  (trigonal field splitting), our measured susceptibilities and anisotropies fit well with the deduced theory<sup>147</sup>, which shows that out of the trigonally split components  ${}^5E$  ( $C_{3v}$ ) and  ${}^5A_1$  ( $C_{3v}$ ) of the ground  ${}^5T_{2g}$  ( $O_h$ ) orbital, doublet  ${}^5E$  lies lowest. This means  $e$  ( $t_{2g}$ ) is lower in energy than  $a$  ( $t_{2g}$ )\*\*. Keeping this in mind we can explain our polarized spectrum if we consider that ligand orbital  $a_1$  ( $t_{2u}$ ) lies lower than  $e$  ( $t_{2u}$ ) (Fig. 14b). The possible

\* The transition cannot be electron transfer from metal to  $Cl^-$  ion, since the electron will have to go to next shell of  $Cl^-$  ion. Further, it cannot be  $t_{1g}$  (ligand)  $\rightarrow$   $t_{2g}$  (metal), since such a transition should be weak compared to  $t_{2u}$  (ligand)  $\rightarrow$   $t_{2g}$  (metal transition). The transition  $t_{1u}$  (ligand)  $\rightarrow$   $t_{2g}$  (metal) is expected to be at higher energies.

\*\*  ${}^5T_{2g}$  ( $O_h$ ) ground state of  $Fe^{2+}$  comes mainly from the  $t_{2g}^4 e_g^2$  configuration. The separation  $\Delta$  between the  ${}^5A$  ( $C_{3v}$ ) and  ${}^5E$  ( $C_{3v}$ ) state (i.e. the two components of ( $O_h$ )  ${}^5T_{2g}$  state) is expected to be almost equal to the orbital energy difference between two components ( $e$  ( $C_{3v}$ ) and  $a$  ( $C_{3v}$ )) of  $t_{2g}$  ( $O_h$ ) orbital split by the original field.

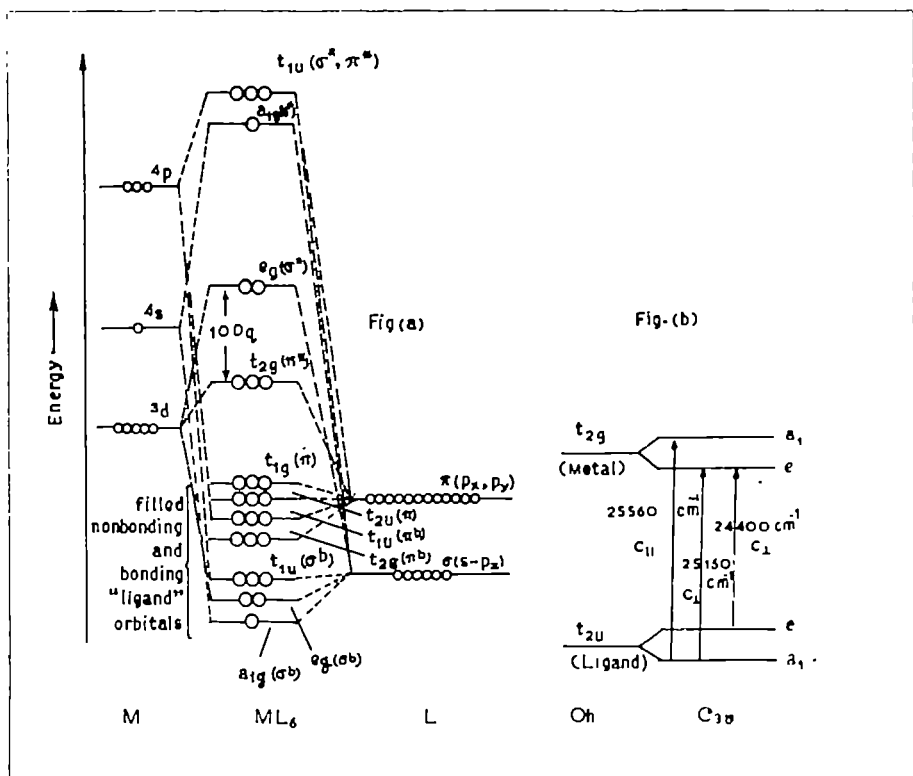


Fig.14(a). Molecular-orbital energy level scheme for an octahedral (ML<sub>6</sub>) complex.

Fig.14(b). Splitting of the t<sub>2g</sub>(metal) and t<sub>2u</sub>(ligand) orbital under C<sub>3v</sub> (Not to scale).

transitions are (in order to decreasing energy)  $a_1 \rightarrow a_1$  ( $\parallel$  polarized),  $a_1 \rightarrow e$  ( $\perp$  polarized),  $e \rightarrow a_1$  ( $\perp$  polarized) and  $e \rightarrow e$  ( $\perp, \parallel$  polarized). From the observed polarized spectra of  $77^\circ\text{K}$  (Fig. 12b), it can be seen that there are two transitions in  $c_1$  direction at  $25160\text{ cm}^{-1}$  and  $24400\text{ cm}^{-1}$  and one transition in  $c_{11}$  direction at higher energy, i.e.  $25560\text{ cm}^{-1}$ . If we assign  $25160\text{ cm}^{-1}$  and  $25560\text{ cm}^{-1}$  to  $a_1(t_{2u}) \rightarrow e(t_{2g})$  and  $a_1(t_{2u}) \rightarrow a_1(t_{2g})$  transition respectively, the magnitude of the trigonal field splittings is found to be roughly  $400\text{ cm}^{-1}$  - a value which is close to our  $\Delta$  value determined from magnetic data.

## II. Magnetic Studies

From our observed values of magnetic anisotropy and susceptibility in the range  $300^\circ\text{K}$  to  $90^\circ\text{K}$ , we have calculated ionic values using Eqns. (75) and (76) and these are given in Table 14 at intervals of  $20^\circ\text{K}$ . The plot of  $\Delta K \cdot T^2$  vs  $T$  and  $\bar{K}$  vs  $T$  are shown in Fig. 15(a) and Fig. 15(b).



Table 14 : Magnetic susceptibility and anisotropy of  $\text{CsCd}_{1-x}\text{Fe}_x\text{Cl}_3$ , where  $x = 3.57$  mol % (graphically interpolated values)

Temperature	$\chi_{\perp} \times 10^6$	$\Delta\chi \times 10^6$	$(K_{\parallel} - K_{\perp}) \times 10^6$	$\bar{K} \times 10^6$
300	12170	933	1400	12480
280	12920	1126	1690	13300
260	13815	1392	2089	14280
240	14760	1759	2639	15350
220	15900	2280	3420	16660
200	17250	2970	4455	18240
180	18870	3990	5985	20200
160	20810	5367	8051	22600
140	23270	7473	11210	25760
120	26500	10800	16200	30100
100	30620	15633	23450	35830
90	33250	18760	28140	39400

A. Ligand Field Energy Levels and the Magnetic Susceptibility

The asymmetry of the ligand field will influence the charge overlap between the central metal ion and the ligands and hence both the spin-orbit coupling constant  $\lambda$  and the orbital reduction factor  $K$  will have anisotropic values<sup>147</sup> In calculating the energies of the lowest orbital triplet  ${}^5T_{2g}$  one can employ the technique of Abragam and Pryce<sup>9</sup> with structural isomorphism between  ${}^5T_{2g}$  and  ${}^5P$ . The effect of admixture of the upper  ${}^5E_g$  state enters through the effective Lande factors  $\alpha_{\parallel}$  and  $\alpha_{\perp}$  ( $\parallel$ ,  $\perp$  to the trigonal axis respectively). Operating with the Hamiltonian

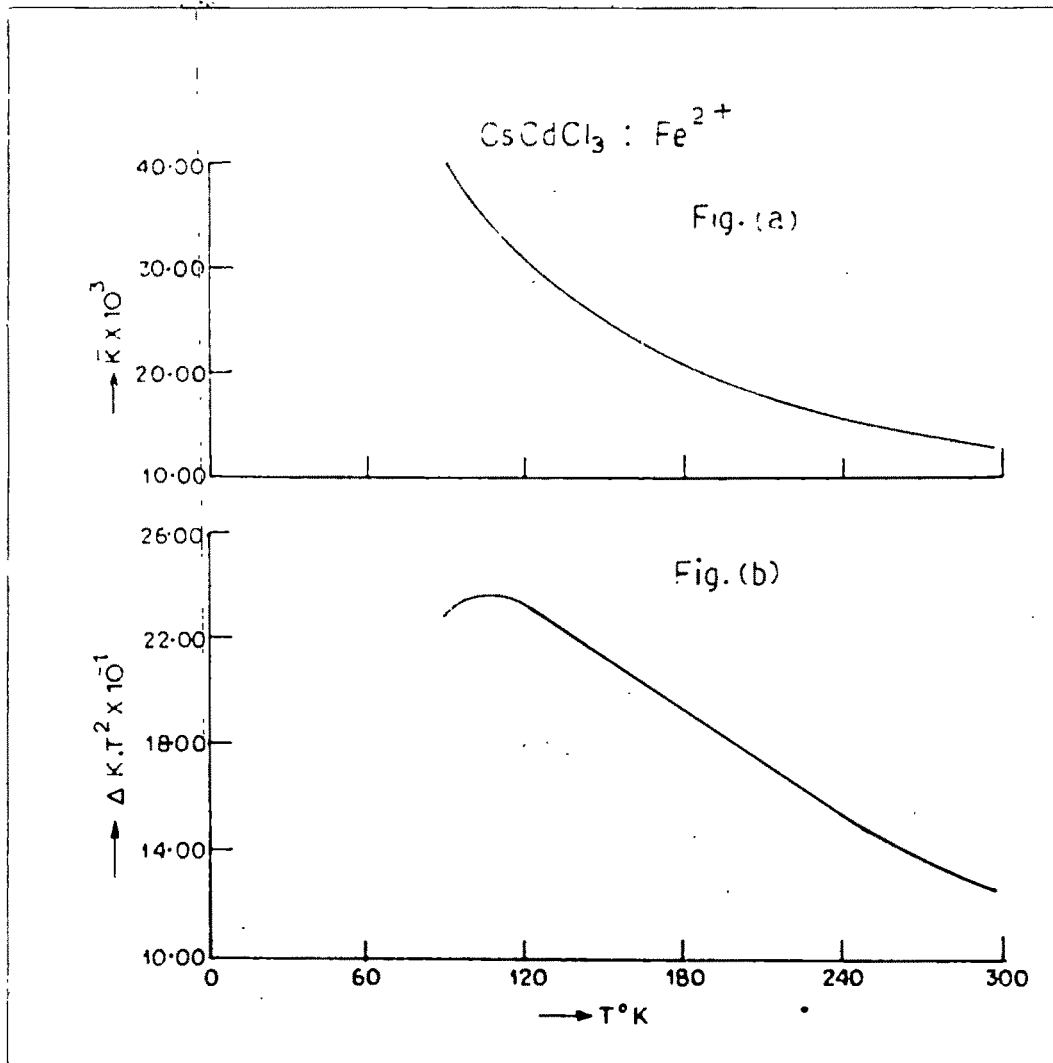


Fig.15(a). Variation of susceptibility ( $\bar{K}$ ) with temperature ( $\text{CsCdCl}_3 : \text{Fe}^{2+}$ )

Fig.15(b). Variation of  $\Delta K.T^2$  with temperature ( $\text{CsCdCl}_3 : \text{Fe}^{2+}$ )

$$H = \Delta (1 - L_z^2) - \alpha_{\parallel} \lambda_{\parallel} L'_z S_z - \alpha_{\perp} \lambda_{\perp} (L'_x S_x + L'_y S_y) \quad (92)$$

on an  $5P$  atomic state, the  $15 \times 15$  energy matrix will break up into two triplets, one quadratic and a singlet and are given by

$m = 0$

	$ -1,1\rangle$	$ 0,0\rangle$	$ 1,-1\rangle$
$ -1,1\rangle$	$\alpha_{\parallel} \lambda_{\parallel}$	$-\sqrt{3} \alpha_{\perp} \lambda_{\perp}$	$0$
$ 0,0\rangle$	$-\sqrt{3} \alpha_{\perp} \lambda_{\perp}$	$\Delta$	$-\sqrt{3} \alpha_{\perp} \lambda_{\perp}$
$ 1,-1\rangle$	$0$	$-\sqrt{3} \alpha_{\perp} \lambda_{\perp}$	$\alpha_{\parallel} \lambda_{\parallel}$

$m = 1$

	$ 1,0\rangle$	$ 0,1\rangle$	$ -1,2\rangle$
$ 1,0\rangle$	$0$	$-\sqrt{3} \alpha_{\perp} \lambda_{\perp}$	$0$
$ 0,1\rangle$	$-\sqrt{3} \alpha_{\perp} \lambda_{\perp}$	$\Delta$	$-\sqrt{2} \alpha_{\perp} \lambda_{\perp}$
$ -1,2\rangle$	$0$	$-\sqrt{2} \alpha_{\perp} \lambda_{\perp}$	$2 \alpha_{\parallel} \lambda_{\parallel}$

$m = 2$

	$ 0,2\rangle$	$ 1,2\rangle$
$ 0,2\rangle$	$\Delta$	$-\sqrt{2} \alpha_{\perp} \lambda_{\perp}$
$ 1,2\rangle$	$-\sqrt{2} \alpha_{\perp} \lambda_{\perp}$	$-\alpha_{\parallel} \lambda_{\parallel}$

$m = 3$

	$ 1,2\rangle$
$ 1,2\rangle$	$-2 \alpha_{\parallel} \lambda_{\parallel}$

(93)

with identical matrices for states with -ve m, solving the secular determinants the eigenvalues are given by<sup>147</sup> .

$$\begin{aligned}
 E_0 &= \frac{1}{2} \left[ (\alpha_{||} \lambda_{||} + \Delta) - \left\{ (\alpha_{||} \lambda_{||} - \Delta)^2 + 24 \alpha_{\perp}^2 \lambda_{\perp}^2 \right\}^{1/2} \right] \\
 E_1 &= \alpha_{||} \lambda_{||} x_1 \\
 E_2 &= \frac{1}{2} \left[ (\Delta - \alpha_{||} \lambda_{||}) - \left\{ (\alpha_{||} \lambda_{||} + \Delta)^2 + 8 \alpha_{\perp}^2 \lambda_{\perp}^2 \right\}^{1/2} \right] \\
 E_3 &= \alpha_{||} \lambda_{||} x_3 \\
 E_4 &= \alpha_{||} \lambda_{||} \tag{94} \\
 E_5 &= \frac{1}{2} \left[ (\Delta + \alpha_{||} \lambda_{||}) + \left\{ (\alpha_{||} \lambda_{||} - \Delta)^2 + 24 \alpha_{\perp}^2 \lambda_{\perp}^2 \right\}^{1/2} \right] \\
 E_6 &= \alpha_{||} \lambda_{||} x_6 \\
 E_7 &= \frac{1}{2} \left[ (\Delta - \alpha_{||} \lambda_{||}) + \left\{ (\Delta + \alpha_{||} \lambda_{||})^2 + 8 \alpha_{\perp}^2 \lambda_{\perp}^2 \right\}^{1/2} \right] \\
 E_8 &= -2 \alpha_{||} \lambda_{||}
 \end{aligned}$$

where  $x_1$ ,  $x_3$  and  $x_6$  are the roots of the cubic eqn.

$$x^3 - x^2(2 + \delta) + (2\delta - 5\rho^2)x + 6\rho^2 = 0 \tag{95}$$

$$\rho = \frac{\alpha_{\perp} \lambda_{\perp}}{\alpha_{||} \lambda_{||}} \quad , \quad \delta = \frac{\Delta}{\alpha_{||} \lambda_{||}} \tag{96}$$

On calculating the magnetic perturbation upto the second order, the principal magnetic susceptibilities are given by

$$\begin{aligned}
 K_{11} = & \frac{N\beta^2}{kZ} \left[ \frac{1}{T} \left\{ \sum_{j=1,3,6} 2 [\alpha_{11} k_{11} (c_j^2 - a_j^2) + 2b_j^2 + 4c_j^2] \exp\left(-\frac{E_j - E_0}{kT}\right) \right. \right. \\
 & + 2 [b_2^2 (2 - \alpha_{11} k_{11}) + 4a_2^2] \exp\left(-\frac{E_2 - E_0}{kT}\right) \\
 & + 2 [a_2^2 (2 - \alpha_{11} k_{11}) + 4b_2^2] \exp\left(-\frac{E_7 - E_0}{kT}\right) \\
 & + 2 [(4 - \alpha_{11} k_{11})^2] \exp\left(-\frac{E_8 - E_0}{kT}\right) \\
 & + 2k \left\{ \frac{2a_0^2 (2 + \alpha_{11} k_{11})^2}{E_4 - E_0} + G_{22}^1 \exp\left(-\frac{E_1 - E_0}{kT}\right) \right. \\
 & + \frac{2a_2^2 b_2^2 (2 + \alpha_{11} k_{11})^2}{E_7 - E_2} \exp\left(-\frac{E_2 - E_0}{kT}\right) + G_{22}^3 \exp\left(-\frac{E_3 - E_0}{kT}\right) \\
 & + G_{22}^4 \exp\left(-\frac{E_4 - E_0}{kT}\right) - \frac{b_6^2 (2 + \alpha_{11} k_{11})^2}{E_5 - E_4} \exp\left(-\frac{E_5 - E_0}{kT}\right) \\
 & \left. + G_{22}^6 \exp\left(-\frac{E_6 - E_0}{kT}\right) - \frac{2a_2^2 b_2^2 (2 + \alpha_{11} k_{11})^2}{E_7 - E_2} \exp\left(-\frac{E_7 - E_0}{kT}\right) \right\}
 \end{aligned} \tag{97}$$

where

$$a_0 = \frac{\sqrt{3} \alpha_{11} \lambda_{11}}{(\alpha_{11} \lambda_{11} - E_0)} b_0 ; \quad 2a_0^2 + b_0^2 = 1 \tag{98}$$

$$a_j = \frac{\sqrt{3}(2\alpha_{11}\lambda_{11} - E_j)}{\sqrt{2}E_j} c_j ; \quad j = 1, 3, 6$$

$$b_j = \frac{2\alpha_{11}\lambda_{11} - E_j}{\sqrt{2}\lambda_{11}} c_j ; \quad a_j^2 + b_j^2 + c_j^2 = 1$$

and  $a_2 = \frac{\sqrt{2}\alpha_{11}\lambda_{11}}{\Delta - E_2} b_2 ; \quad a_2^2 + b_2^2 = 1$

and the partition sum,  $Z$  is given by

$$\begin{aligned} Z = & \left[ 1 + 2 \exp\left(-\frac{E_1 - E_0}{kT}\right) + 2 \exp\left(-\frac{E_2 - E_0}{kT}\right) + 2 \exp\left(-\frac{E_3 - E_0}{kT}\right) \right. \\ & + \exp\left(-\frac{E_4 - E_0}{kT}\right) + \exp\left(-\frac{E_5 - E_0}{kT}\right) + 2 \exp\left(-\frac{E_6 - E_0}{kT}\right) \quad (99) \\ & \left. + 2 \exp\left(-\frac{E_7 - E_0}{kT}\right) + 2 \exp\left(-\frac{E_8 - E_0}{kT}\right) \right] \end{aligned}$$

and the  $G_{\Lambda}$  are given by

$$G_{2Z}^1 = R_{31} + R_{61} ; \quad G_{2Z}^3 = -R_{31} + R_{63}$$

$$G_{2Z}^6 = -R_{63} - R_{61} ; \quad G_{2Z}^0 = -\frac{2a_0^2(2 + \alpha_{11}k_{11})^2}{E_4 - E_0} + \frac{b_0^2(2 + \alpha_{11}k_{11})^2}{E_5 - E_4}$$

$$R_{ij} = \frac{2[\alpha_{11}k_{11}(c_i c_j - a_i a_j) + 2b_i b_j + 4c_i c_j]^2}{E_i - E_j} \quad (100)$$

$$\begin{aligned}
 K_{\perp} = & \frac{2N\beta^2}{Z} \left[ G_{2x}^0 + G_{2x}^1 \exp\left(-\frac{E_1 - E_0}{kT}\right) + G_{2x}^2 \exp\left(-\frac{E_2 - E_0}{kT}\right) \right. \\
 & + G_{2x}^3 \exp\left(-\frac{E_3 - E_0}{kT}\right) + G_{2x}^4 \exp\left(-\frac{E_4 - E_0}{kT}\right) \\
 & + G_{2x}^5 \exp\left(-\frac{E_5 - E_0}{kT}\right) + G_{2x}^6 \exp\left(-\frac{E_6 - E_0}{kT}\right) \\
 & \left. + G_{2x}^7 \exp\left(-\frac{E_7 - E_0}{kT}\right) + G_{2x}^8 \exp\left(-\frac{E_8 - E_0}{kT}\right) \right] \quad (101)
 \end{aligned}$$

where

$$\begin{aligned}
 G_{2x}^0 &= \frac{2A_{01}^2}{E_1 - E_0} + \frac{2A_{03}^2}{E_3 - E_0} + \frac{2A_{06}^2}{E_6 - E_0} \\
 G_{2x}^1 &= -\frac{2A_{01}^2}{E_1 - E_2} + \frac{2B_{21}^2}{E_2 - E_1} + \frac{2A_{41}^2}{E_4 - E_1} + \frac{2A_{51}^2}{E_5 - E_1} + \frac{2B_{71}^2}{E_7 - E_1} \\
 G_{2x}^2 &= -\frac{2B_{21}^2}{E_2 - E_1} + \frac{2B_{23}^2}{E_3 - E_2} + \frac{2B_{26}^2}{E_6 - E_2} + \frac{2(2b_2 - \alpha_{\perp} K_{\perp} a_2 / \sqrt{2})^2}{E_8 - E_2} \\
 G_{2x}^3 &= -\frac{2A_{03}^2}{E_3 - E_0} - \frac{2B_{23}^2}{E_3 - E_2} + \frac{2A_{43}^2}{E_4 - E_3} + \frac{2A_{53}^2}{E_5 - E_3} + \frac{2B_{73}^2}{E_7 - E_3} \\
 G_{2x}^4 &= -\frac{2A_{41}^2}{E_4 - E_1} - \frac{2A_{43}^2}{E_4 - E_3} + \frac{2A_{46}^2}{E_6 - E_4} \\
 G_{2x}^5 &= -\frac{2A_{51}^2}{E_5 - E_1} - \frac{2A_{53}^2}{E_5 - E_3} + \frac{2A_{56}^2}{E_6 - E_5}
 \end{aligned}$$

$$\begin{aligned}
 G_{2x}^6 &= -\frac{2A_{06}^2}{E_6 - E_0} - \frac{2B_{26}^2}{E_6 - E_2} - \frac{2A_{46}^2}{E_6 - E_4} - \frac{2A_{56}^2}{E_6 - E_5} + \frac{2B_{76}^2}{E_7 - E_6} \\
 G_{2x}^7 &= -\frac{2B_{71}^2}{E_7 - E_1} - \frac{2B_{73}^2}{E_7 - E_3} - \frac{2B_{76}^2}{E_7 - E_6} + \frac{2(2a_2 - \alpha_{\perp} k_{\perp} b_2 / \sqrt{2})^2}{E_8 - E_7} \\
 G_{2x}^8 &= -\frac{2(2a_2 + \alpha_{\perp} k_{\perp} b_2 / \sqrt{2})^2}{E_8 - E_7} - \frac{2(2b_2 - \alpha_{\perp} k_{\perp} a_2 / \sqrt{2})^2}{E_8 - E_2}
 \end{aligned} \tag{102}$$

where

$$\begin{aligned}
 A_{0j} &= \sqrt{6}(a_0 a_j + b_0 b_j) - \left(\frac{\alpha_{\perp} k_{\perp}}{\sqrt{2}}\right)(a_j b_0 + b_j a_0) + 2c_j a_0 \\
 B_{2j} &= (\sqrt{6} b_2 a_j + 2a_2 b_j) - \left(\frac{\alpha_{\perp} k_{\perp}}{\sqrt{2}}\right)(b_2 b_j + a_2 c_j) \\
 A_{4j} &= \sqrt{3} a_j + \alpha_{\perp} b_j k_{\perp} / 2 - \sqrt{2} c_j \\
 A_{5j} &= \sqrt{3}(b_0 a_j - 2a_0 b_j) - (\alpha_{\perp} k_{\perp} / 2)(b_0 b_j - 2a_0 a_j) + \sqrt{2} b_0 c_j \\
 B_{7j} &= (\sqrt{6} a_2 a_j - 2b_2 b_j) - (\alpha_{\perp} k_{\perp} / \sqrt{2})(b_j a_2 - c_j b_2)
 \end{aligned} \tag{103}$$

### B. Parametric Fittings and Discussion of the Experimental Results

As in the case of  $\text{CsCdCl}_3 : \text{Co}^{2+}$ , we obtained by trial and error a set of values for  $\alpha_{\parallel} k_{\parallel}$ ,  $\alpha_{\perp} k_{\perp}$ ,  $\alpha_{\parallel} \lambda_{\parallel}$ ,  $\alpha_{\perp} \lambda_{\perp}$  and  $\Delta$ , which gives best fit with our anisotropy and susceptibility data (Table 15). In the process of fitting, we have seen that +ve values of  $\Delta$  fits our magnetic data more closely with the theory, thereby indicating that the doublet lies lowest. The value of  $\Delta$  seems to be near  $320 \text{ cm}^{-1}$ . The small value of  $\Delta$ , both from the observation of  $\text{Co}^{2+}$  and  $\text{Fe}^{2+}$  indicates that the trigonal field strength in  $\text{CsCdCl}_3$  is rather small. The anisotropic reduction of the spin orbit coupling



constant and the orbital reduction parameter  $K$  give evidence of a fair degree of metal-ligand charge overlap. In the parametric fittings we choose the values of the parameters for  $90^\circ\text{K}$  and it is seen that with these parameters the difference between observed and calculated values differ from  $\sim 0.25\%$  to  $\sim 4\%$  for  $\bar{K}$  and  $\sim 1\%$  to  $\sim 4.2\%$  for  $\Delta K$  as we go up. These variations may be due to the fact that we have tried to fit our data with same value of the parameters throughout the whole range of temperature as in the case of  $\text{Co}^{2+}$ , which is not strictly correct. The fine structure energy levels of  $^5\text{T}_2$  state from our magnetic calculation are given in Fig. 15c.

Table 15 : Results of Parametric Fittings \*

$$\begin{aligned} \alpha_{\parallel} \lambda_{\parallel} &= -86.5 \text{ cm}^{-1} & \alpha_{\perp} \lambda_{\perp} &= -80 \text{ cm}^{-1} \\ \alpha_{\parallel} k_{\parallel} &= .6 & \alpha_{\perp} k_{\perp} &= .8 \\ \Delta &= +320 \text{ cm}^{-1} \end{aligned}$$

Temperature $^\circ\text{K}$	$\Delta K \times 10^6$	$\bar{K} \times 10^6$
300	11346 (1400)	12008 (12480)
240	2705 (2639)	15008 (15350)
180	6099 (5985)	20008 (20200)
120	16012 (16200)	29871 (30100)
90	28437 (28140)	39289 (39400)

\* Experimental values are in parenthesis.

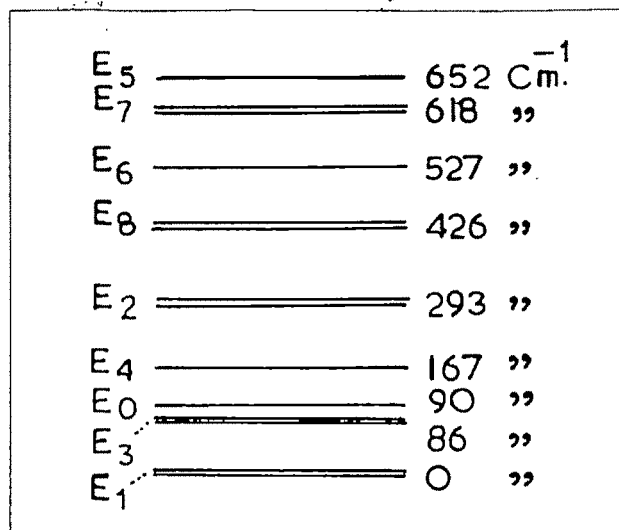


Fig.15(c). Fine structure energy level scheme ground  ${}^5T_2$  state of  $CsCdCl_3 : Fe^{2+}$  with  $\Delta = +320 \text{ cm}^{-1}$  from our magnetic calculation (Not to scale).

The g-values :

As it has been seen that the lowest level is a doublet  $|\pm 1\rangle$  ; the g-values are given by<sup>11</sup>

$$g_{\parallel} = 2 |\langle \Psi_+ | -\alpha_{\parallel} K_{\parallel} L'_z + 2S_z | \Psi_+ \rangle|$$

$$g_{\perp} = 2 |\langle \Psi_+ | -\alpha_{\perp} K_{\perp} L'_x + 2S_x | \Psi_+ \rangle|$$

On performing calculations, we find

$$g_{\parallel} = 2 [(4 + \alpha_{\parallel} K_{\parallel}) c_1^2 + 2b_1^2 - \alpha_{\parallel} K_{\parallel} a_1^2]$$

$$g_{\perp} = 0$$

and use of our magnetic data in above equations yields

$$g_{\parallel} = 6.663 \text{ and } g_{\perp} = 0.$$